Numerical Simulations for Electromagnetic Processes in the Earth

Project Representative
Yozo Hamano — Institute for Research on Earth Evolution, Japan Agency for Marine-Earth Science and Technology

Authors
Futoshi Takahashi — Department of Earth and Planetary Sciences, School of Science and Engineering, Tokyo Institute of Technology
Takatoshi Yanagisawa — Institute for Research on Earth Evolution, Japan Agency for Marine-Earth Science and Technology
Takao Koyama — Earthquake Research Institute, The University of Tokyo
Yozo Hamano — Institute for Research on Earth Evolution, Japan Agency for Marine-Earth Science and Technology

Convective motions in the Earth's outer core are generally driven by the buoyancy arising from thermal and chemical effects, which are closely related with the origin, composition and thermal history of the Earth. To better understand the thermo-chemical evolution of the Earth's core and its relation with the geomagnetic field generation, we performed numerical simulations of the geodynamo powered by double diffusive convection. We find that the morphology of the magnetic field is determined by the dynamic ratio of the two driving mechanisms. A dipolar magnetic field is maintained as long as the power injected by compositional buoyancy comprises at least 30-40% of the total.

As an important basic process for liquid metal convection, we studied the variation of flow pattern in the presence of magnetic field. We recognized five flow regimes depending on Rayleigh number and intensity of the magnetic field. They are consistent with laboratory experiments, and we provide a quantification of the effect of magnetic field on flow pattern.

We also performed electromagnetic induction studies to elucidate the electrical conductivity structure in the mantle beneath Australia by using the geomagnetic data on the land. As the results, the very-highly conductive region as much as 1 S/m was found in the mid-mantle of the southeastern region of Australia. This probably happened by enhancement of water content due to the dehydration of the stagnant slab.

Keywords: Geodynamo, Geomagnetic field, Core convection, Magnetohydrodynamics, Electrical conductivity of mantle

1. Introduction

Internal activities of the Earth are the consequence of convective motions of the mantle and core. The convection of mantle and core also control Earth's surface environment through material circulations, volcanism, continental drift, geomagnetic field, and so on. The mantle convection, driven by both cooling of the Earth and internal radiogenic heating, takes the form of rigid-plate motions at the surface, and sometimes leads to disastrous earthquakes. As the mantle cools, the underlying liquid metallic core becomes thermally unstable and the resulting convective motion causes generation of the geomagnetic field and its time variations. As a result of cooling of the liquid core containing some lighter elements, a solid denser inner core grows from below, causing compositional instability in the liquid outer core. The geomagnetic field has been monitored at the surface or from satellites. It contains some information on both the core convection and the electrical conductivity of the mantle. Our purpose is to construct a comprehensive view on these interior dynamics and electromagnetic processes. Our group has made efforts to understand the structure and dynamics of the Earth's deep interior by means of realistic numerical modeling of the core and mantle convection. We report here the progress on three topics, core dynamo simulation with thermal and compositional convection, liquid metal convection under a magnetic field, and the electrical conductivity structure of mantle.

2. Geodynamo simulations with double diffusive convection

Convective motion in the Earth's outer core is considered

to be the most likely source for the generation and sustenance of the geomagnetic field via a dynamo mechanism. In the Earth's core, convection is driven by thermal and compositional buoyancy. Thermal convection is driven by the super-adiabatic part of the temperature gradient within the core coming from secular cooling of the core, latent heat release due to solidification of iron at the inner core boundary. Compositional convection is powered by the ejection of light elements into the outer core at the inner core boundary.

Based on the molecular values, the thermal Prandtl number Pr^T = O(0.1), while the compositional Prandtl number Pr^C = O(10^2). In spite of such a big difference in the Prandtl number, based on the assumption of turbulent diffusivity due to turbulence in the core, the same values of thermal and compositional Prandtl numbers has been taken. Then, temperature and composition are combined into one variable called codensity [1]. However, applicability of the codensity treatment to the Earth's core is not evident, because we have little knowledge on core turbulence. Here, we employ a double diffusive convection (DDC) model to investigate the effects of co-existence of two driving force at different Prandtl numbers on the core convection and the geodynamo. In the codensity treatment, it is impossible to discriminate contributions from the two agents to the dynamics of convection, while the DDC model allows us to independently examine the effects of thermal and compositional convection.

By extending our code [2, 3], numerical simulations of DDC are performed at the Ekman number, $E = 3\times10^{-4}$, and 10^{-4}, whereas the Prandtl numbers are fixed at Pr^T = 0.1, Pr^C = 1 and Pm = 3, where Pm is the magnetic Prandtl number. The Ekman number adopted here is not extremely low, because we put emphasis on parameter survey to capture a gross behavior in terms of thermal and compositional forcing. Varying the two Rayleigh numbers representing strength of thermal (Ra^T) and compositional (Ra^C) forcing, we have obtained dipolar and non-dipolar dynamos. In Fig. 1 the resultant structures of convection and magnetic field are displayed. The non-dipolar dynamos appear when thermal convection is dominant over compositional convection, while the dipolar dynamos are preferred in the opposite situation. Moreover, the flow structures, which should be responsible for such different magnetic field morphology, are distinct between these cases. The cyclonic vortices are significantly larger than the anti-cyclones in the non-dipolar dynamos. On the other hand, two kinds of vortex are comparable with each other in the dipolar dynamos.

The dipolar and non-dipolar dynamos are distinguished by strength of the zonal flows. The non-dipolar dynamos tend to show larger fractions of the zonal flow kinetic energy to the total kinetic energy than the dipolar dynamos. The threshold value seems about 12%. Then, the zonal flow power budget is investigated according to Aubert [4]. As a result, two dynamic regimes are confirmed. One is found to be in a balance between the Coriolis and Lorentz force terms, namely a magnetostrophic balance, and the other is in a balance between the Coriolis and Reynolds stress (inertial) terms. Figure 2 shows dominant contributions to the power budget and the resultant zonal flow. In the magnetostrophic state (Fig. 2a), both the Coriolis and Lorentz forces act to enhance and drain the energy of the zonal flow. In this case, the magnetic field enters into thermal wind balance to oppose the Coriolis force. Due to the braking effects of the Lorentz force, the growth of the zonal flow is suppressed and the zonal flow kinetic energy is forced to be small. On the other hand, in case of a non-dipolar dynamo (Fig. 2b), the

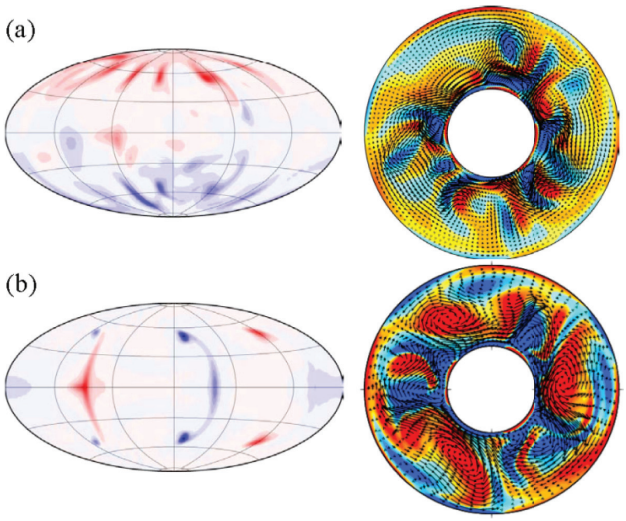

Fig. 1 Typical simulation results for (a) dipolar dynamo and (b) non-dipolar dynamo. The radial magnetic field at the core surface (left) and the axial vorticity and the horizontal flow vectors on the equatorial plane (right). Positive (negative) values are denoted in red (blue).

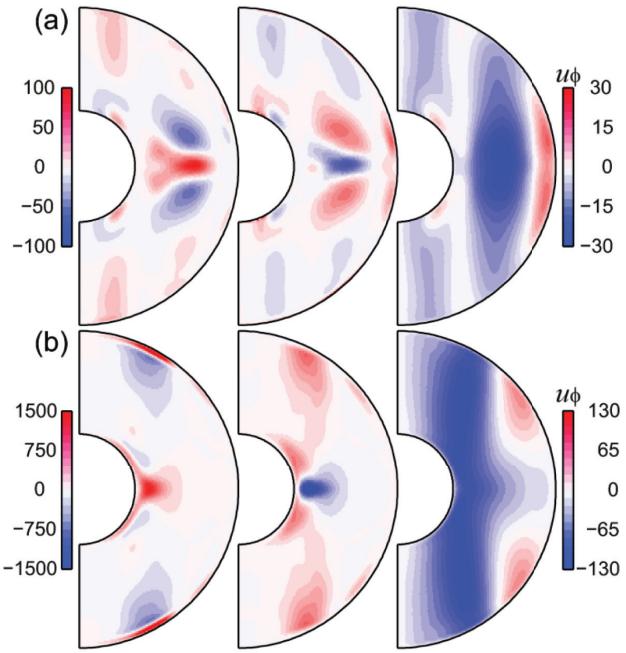

Fig. 2 Zonal flow power budget at $E = 3 \times 10^{-4}$ for (a) dipolar dynamo and (b) non-dipolar dynamo. Time-averaged contributions from the Coriolis force (left), Lorentz force in (a) and Reynolds stress term in (b) (center), and the zonal flow (right) are represented.

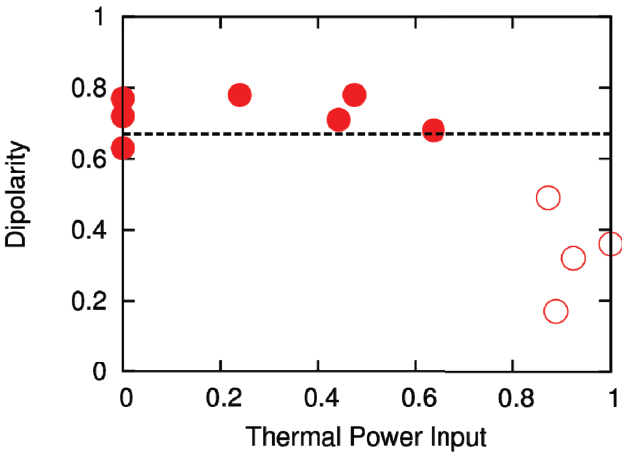

Fig. 3 Dipolarity vs. thermal power input rate at $E = 3 \times 10^{-4}$. The dipolar (non-dipolar) dynamos are represented by filled (open) circles.

inertial term plays a role as the main source of the zonal flow. The zonal flow aligned with the z-axis shows a typical pattern strongly constrained by the Taylor-Proudman theorem. Such a flow structure is well correlated with the Reynolds stress [4]. It is thus suggested that the larger fraction of the zonal flow is a result of this force balance.

To examine which source of convection and dynamo action is dominant for a given pair of Ra^T and Ra^C, we calculate the power injection rate, the dot product of the velocity field and each buoyancy force integrated over the shell volume. Figure 3 is a plot of dipolarity (the ratio of the dipole component to the total field strength at the core surface up to spherical harmonic degree 12) with respect to thermal power injection to the total injection (Ftc). It is evident that the two dynamo regimes are distinctly separated at Ftc ~ 0.65. It is indicated that the dipolar dynamos are maintained if the compositional buoyancy accounts for at least 30-40% of the total kinetic energy input. It is thus suggested that the present dipolar geodynamo is fueled compositionally by at least 30%.

3. Liquid-metal thermal convection in the presence of a magnetic field

The study on the nature of thermal convection in liquid metals under a magnetic field is important for the dynamics of Earth's metallic cores. Electric current is induced when a flow of liquid metal crosses a magnetic field, and it generates Lorentz force. The Lorentz force changes the force balance, making the flow behavior different from no-magnetic field situations. In general, viscosity of liquid metals is very low and their flow easily becomes turbulent, but when a magnetic field is applied on liquid metals, it makes anisotropic flow structure with suppression of turbulence depending on its direction and intensity. Here we provide fundamental dataset for realistic liquid metal convection. To quantify the effect of magnetic field on flow patterns, we performed laboratory experiments [5] and

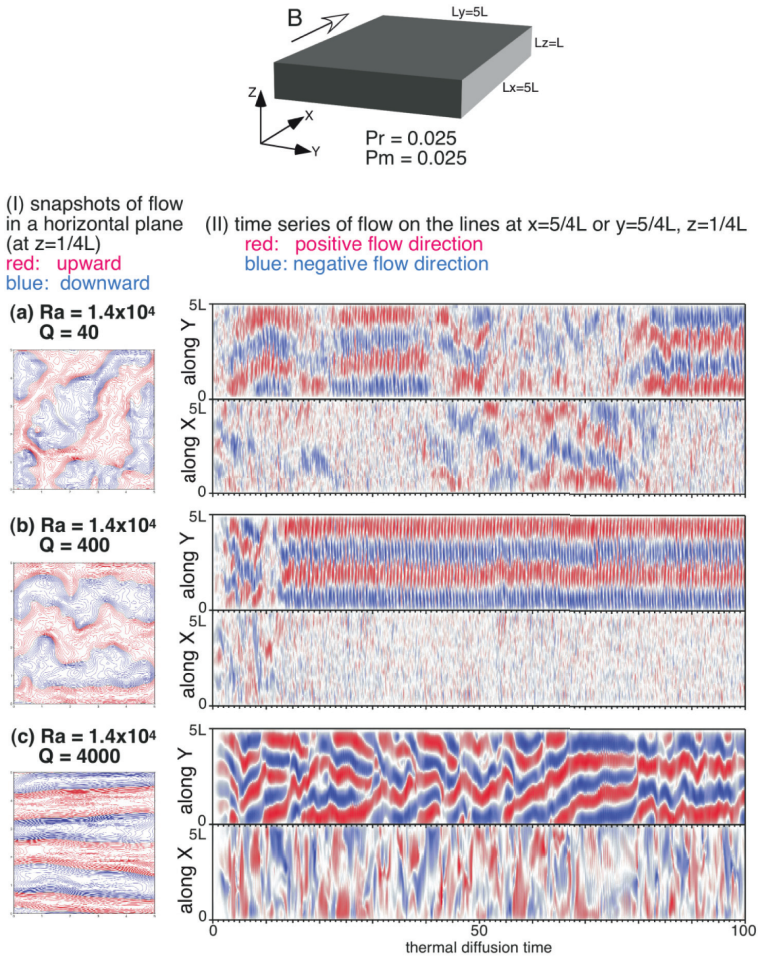

Fig. 4 Setting and result of numerical simulations for liquid metal convection under several intensities of uniform horizontal magnetic field. The variation of pattern depending on Q is displayed here, with Ra fixed at 1.4×10^4. Pr and Pm of the fluid are 0.025. In the left side square boxes, the contours are flow velocity in vertical direction; red indicates the upward flow, and blue indicates downward flow. The right rectangular boxes show the time variations of horizontal flow along X and Y lines; red (blue) indicates positive (negative) flow direction. (a) regime (1) in the main text: isotopic large-scale cell, (b) regime (3): short period oscillatory behavior of rolls, and (c) regime (4): continuous transitions between roll numbers.

numerical simulations on Rayleigh-Benard convection by liquid metal, with various intensities of a uniform horizontal magnetic field B. In the numerical simulations, both the Prandlt number and magnetic Prandtl number of the working fluid are set small to simulate liquid metals. Our numerical result successfully reproduced most of the behaviors observed in the laboratory experiments.

We recognized five flow regimes depending on Ra and Q (Q: Chandrasekhar number, proportional to the square of B), that is, (1) isotropic large-scale cell pattern, (2) anisotropic cell with larger flow velocity perpendicular to B, (3) short-period oscillatory behavior of rolls aligned in the direction of B, (4) continuous transitions between roll numbers in the vessel, and (5) steady 2-D rolls. In (4), reversals of the flow direction in rolls were observed several times. These behaviors are summarized as a regime diagram of convection patterns in relation to Ra and Q. The key mechanisms for the variation are the enhancement of two-dimensionality and increase of roll number for larger Q situations. These flow regimes can be classified by Ra/Q, that is the ratio of buoyancy force to the Lorentz force. If buoyancy force is much larger than Lorentz force, the flow is turbulent and isotropic structure is dominant. Short-period of oscillation (3) is observed where the ratio Ra/Q is lower than 100. Continuous transitions of roll numbers (4) are observed at Ra/Q between 10 and 30, and convection pattern keeps steady roll (5) at Ra/Q smaller than 10. This relation is valid for wide parameter ranges.

4. Electrical Conductivity Structure in the mantle beneath Australia

We present the three-dimensional electrical conductivity in the mid-mantle beneath Australia. We performed the electromagnetic induction studies by using the C-responses data at the 8 stations in Australia, which are published by [6]. The period range to be used is between 4 and 100 days. These data are inverted to the electrical conductivity structure by using the method in [7], which used the modified IDM (e.g. [8]) for forward modeling and the adjoint approach and the quasi-Newton method for inverse modeling to make the calculation drastically fast. To make the numerical results precise, the topmost thin layer is input for strong contrast of the electrical conductivity between ocean and land with 1 degree interval horizontally. A P10 external source is input in the geomagnetic coordinate, as the auroral effect is supposed to be weak in the mid-latitude region like this paper.

The results are shown in the Fig. 5. You can see the very-highly conductive region in the mid-mantle (depth: 520-660km), corresponding as much as 1 S/m. Resolution checks made them sure the existence of the conductive body. This conductive body probably happened by enhancement of water content due to the dehydration of the stagnant slab. The seismological structures also support the slow region of the seismic wave in this region (e.g. [9]). These enhancements also appear beneath the Pacific [10]. This means the cold plate such like the Pacific plate can carry water deep in the mid-mantle, and it can be a big reservoir of water.

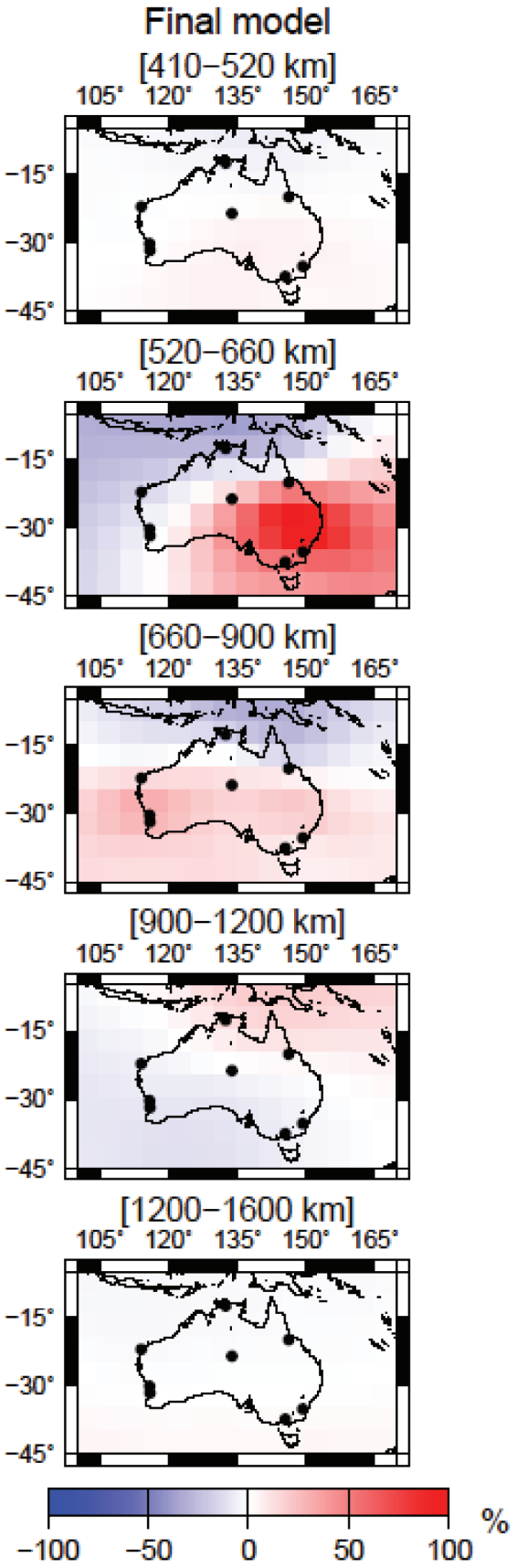

Fig. 5 Three-dimensional electrical conductivity perturbation beneath Australia.

Acknowledgement

On the induction study, the authors sincerely thank Amir Khan and Alexey Kuvshinov in ETH Zurich for fruitful discussion on the numerical results.

References

[1] S. I. Braginsky and P. H. Roberts, “Equations governing convection in Earth’s core and the geodynamo”, *Geophys. Astrophys. Fluid Dyn*., 79, 1–97, 1995.

[2] F. Takahashi, “Implementation of a high-order combined compact difference scheme in problems of thermally driven convection and dynamo in rotating spherical shells”, *Geophys. Astrophys. Fluid Dyn*., 106, 231-249, 2012.

[3] F. Takahashi and H. Shimizu, “A detailed analysis of a dynamo mechanism in a rapidly rotating spherical shell”, *J. Fluid. Mech*., 701, 228-250, 2012.

[4] J. Aubert, “Steady zonal flows in spherical shell dynamos”, *J. Fluid Mech*., 542, 53–67.

[5] T. Yanagisawa, Y. Yamagishi, Y. Hamano, Y. Tasaka, and Y. Takeda, “Spontaneous flow reversals in Rayleigh-Bénard convection of a liquid metal”, *Phys. Rev. E* 83, 036307, 2011.

[6] A. Semenov and A. Kuvshinov, “Global 3-D imaging of mantle conductivity based on inversion of observatory C-responses – II. Data analysis and results”, *Geophys. J. Int*., 191, 965-992, 2012.

[7] T. Koyama, “A study on the electrical conductivity of the mantle by voltage measurements of submarine cables”, PhD thesis, University of Tokyo, 2001.

[8] O. Pankratov, D. Avdeev, and A. Kuvshinov, “Electromagnetic field scattering in a homogeneous Earth: a solution to the forward problem”, *Phys. Solid Earth*, 31, 201-209, 1995.

[9] J. Ritsema, H. J. van Heijst, A. Deuss, and J. H. Woodhouse, “S40RTS: a degree-40 shear-velocity model for the mantle from new Rayleigh wave dispersion, teleseismic traveltimes, and normal-mode splitting function measurements”, *Geophys. J. Int*., 184, 10.1111/j.1365-246X.2010.04884.x, 2011.

[10] T. Koyama, H. Shimizu, H. Utada, M. Ichiki, E. Ohtani, and R. Hae, “Water content in the mantle transition zone beneath the north Pacific derived from the electrical conductivity anomaly”, in *Earth’s Deep Water Cycle, AGU Geophysical Monograph*, vol. 168, pp. 171-179, American Geophysical Union, 2006.

地球内部の電磁気過程に関する数値シミュレーション

プロジェクト責任者
浜野　洋三　　海洋研究開発機構　地球内部ダイナミクス領域
著者
高橋　　太　　東京工業大学　大学院理工学研究科　地球惑星科学専攻
柳澤　孝寿　　海洋研究開発機構　地球内部ダイナミクス領域
小山　崇夫　　東京大学　地震研究所
浜野　洋三　　海洋研究開発機構　地球内部ダイナミクス領域

地球の冷却に起因するマントル対流とコア対流は、固体地球上に生起する諸々の自然現象の原因をつかさどる根本的な物理プロセスであるとともに、この両者は様々な関係で結合している。コアの対流により地磁気が生成・維持されることで、表層環境が穏やかに保たれてきた一方、このコアの冷却を支配するのは周囲のマントルである。更には、地表で観測される電磁場はマントルの電気伝導度を反映したものである。われわれはこれまで、マントルとコアという２つの対流系を、より実際の地球に近い条件のもとで、数値的にモデリングする研究をおこなってきた。また、マントルの電気伝導度構造の推定結果が得られるようになったので、これらを報告する。

地球のコアでは、内核成長にともない軽元素が液相に濃集する結果、組成対流もおこっていると考えられる。これをふまえてダイナモシミュレーションにおいて、熱対流と組成対流を二重拡散対流として同時に取り扱うようにコードを改良した。そのコードを用いて、エクマン数を 3×10^{-4}、熱プラントル数 0.1、組成プラントル数 1.0、磁気プラントル数 3.0 としてダイナモシミュレーションを実施した。パラメータサーベイの結果、双極子的なダイナモと非双極子的なダイナモが得られたが、どちらが実現するかは組成による浮力と熱による浮力のダイナミックな割合によって決まることがわかった。

一方、実際の液体金属において熱プラントル数は 10^{-2}、磁気プラントル数は 10^{-6} と小さいのが特徴で、それほど小さな値を用いることのできないダイナモシミュレーションとの間をつなぐ必要がある。コアの乱流的なふるまいをよりよく理解するために、液体金属のベナール対流の室内実験をおこない、それをさらに数値的にモデリングした。矩形領域内での液体金属の熱対流シミュレーションにおいて、熱プラントル数を実際の物性値である 0.025、磁気プラントル数を 0.025 から 10^{-4} まで小さくして、磁場の影響下での熱対流の性質を調べた。室内実験で得られている対流パターンとその時間変動を再現することに成功した。

マントルの電気伝導度およびその不均質性はマントルの構造を推定するのに重要な情報を与える。電気伝導度はメルトや水の分布に敏感であるため、地震波速度と組み合わせることで不均質性の原因を特定することが可能となる。磁場変動に伴う応答を地表で観測することにより、マントルの電気伝導度を知ることが出来る。陸上観測点での地磁気データを利用して、オーストラリア大陸下マントルの三次元電気伝導度構造の推定をおこなった。その結果、オーストラリアの南東にあたる領域のマントル遷移層が著しい高電気伝導異常を示すことがわかった。地震波速度構造とあわせて吟味すると、高電気伝導の原因は沈み込んだスラブからの脱水によるものと考えられる。

キーワード: 地球ダイナモ, 地磁気, コア対流, 磁気流体力学, マントル電気伝導度構造